ARMA 22–777

The Effect of Rock Anisotropy on Hydraulic Fracture Containment in The Bakken Formation

Chellal, H.A.K. and Merzoug, A.
University of North Dakota, Grand Forks, North Dakota, United States
Rasouli, V.
University of North Dakota, Grand Forks, North Dakota, United States
Brinkerhoff, R.
Wastach Energy Management, Provo, Utah, United States

ABSTRACT: In this study, a special focus was dedicated to the effect of elastic anisotropy of shales on the in-situ stress contrast between different layers and its implications on the vertical containment of hydraulic fractures (HF) and how they relate to the widely observed fracture driven interaction (FDI) phenomena and undesirable HF height growth. The reported elastic and mechanical properties of the main members of the Bakken petroleum system in the Williston Basin (i.e. Upper and Lower Bakken Shale, Middle Bakken and Three Forks) (Ellafi et al., 2019) was used to estimate the in-situ stresses based on anisotripic rock properties and use the minimum horizontal stress profile for HF modeling. The estimated stress profile appeared to be very different from the one calculated based on the isotropic formation assumption. The anisotropic stress model, as reported by other researchers, is more realistic in transverse istorpic rocks and rock with high volume of clay and TOC and generated more reliable results that conform better with other indicators and observations from other types of data associated with HF geometry.

1. INTRODUCTION

Accurate estimation of the minimum principal in situ stress is a milestone in the successful design of hydraulic fracturing (HF) jobs (Ganpule et al., 2015). The role of accurate stress variations with depth becomes more pronounced where HF is performed in different horizons to explore what is called stacked pay. Estimation of in-situ horizontal stresses are mainly attributed to the inherently simplistic assumptions of the commonly used stress models (Zoback, 2007). However, the revolution in oil and gas due to production from Shale plays indicated the necessity of using anisotropic, or what is so-called as transverse isotropic (TI) assumption for the formation for estimation of horizontal stresses. In this study, we showcased the importance of laboratory characterization of the elastic and mechanical properties for accurate prediction of stress profiles and how they can change our designs and improve the profitability of our investments by generating more reliable stress models that are coherent with what is indicated by other types of data. This can serve as a strong base for improved planning. This is proved through our case study on performed using data from the Bakken formation in the Williston Basin petroleum system, where the use of a well-calibrated anisotropic stress model proved to strongly agree with HF geometries observations from microseismic data reported in many other studies such as McKimmy et al. (2022) and Lorwongngam et al. (2018).

2. BAKKEN GEOLOGY

The Bakken petroleum system is mainly composed of the Devonian Three Forks Formation, And Devonian early Mississippian Bakken formation (Anna et al., 2010). The Bakken is subdivided into three members ordered from top to bottom: Upper Bakken Shale, Middle Bakken, and Lower Bakken Shale (LEFEVER, J. A., North Dakota Geolog, 1992). Consistent with the Bakken formation, Three Forks also is subdivided into three members as Upper Three Forks, Middle Three Forks and Lower Three Forks (Sonnenberg et al., 2011)

In this unconventional petroleum system, it is believed that the source rocks are the Upper and Lower Bakken Shales, where high organic matter content is usually observed. The maturated hydrocarbons then migrated to

the Middle Bakken and Upper Three Forks (Pitman et al., 2012). Horizontal drilling and HF in the Bakken petroleum system usually targets the latter mentioned formations due to their desirable characteristics (porosity, permeability, brittle behavior) compared to the shaly members.

3. ELASTIC PROPERTIES ESTIMATION AND CALIBRATION

core depth). It was assumed that the medium is vertical transversely isotropic (VTI), and based on that, the vertical dynamic properties were converted to static elastic properties using the results from the cores that were drilled perpendicularly to the bedding planes, and the horizontal dynamic properties were converted to static using the results on cores drilled parallel to the bedding planes. Noticeable differences were observed where the clay and organic-rich members were highly anisotropic, in contrast to those that had low clay and kerogen content

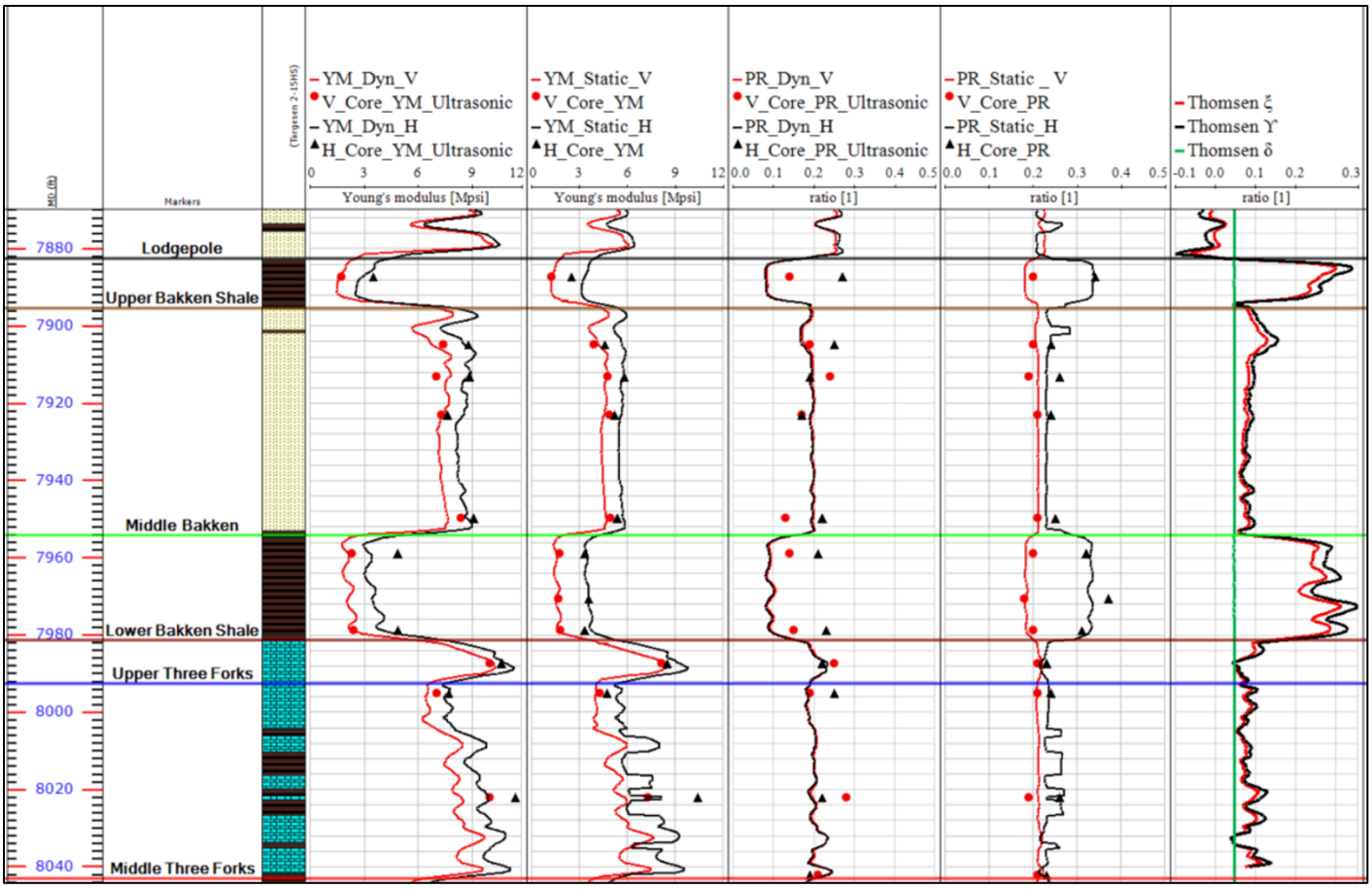

Fig. 1. Dynamic and Elastic properties of the Bakken Petroleum System in the study well. (**YM_Dyn_V**: vertical dynamic Young's modulus; **V_Core_YM_Ultrasonic**: vertical core ultrasonic Young's modulus; **YM_Dyn_H**: horizontal dynamic young's modulus; **H_Core_YM_Ultrasonic**: horizontal core ultrasonic Young's modulus **YM_Static_V**: vertical static Young's Modulus; **V_Core_YM**: vertical core static Young's modulus; **YM_Static_H**: horizontal static young's modulus; **H_Core_YM**: horizontal core static Young's modulus; **PR_Dyn_V**: vertical dynamic Poisson's ratio; **V_Core_PR_Ultrasonic** : vertical core ultrasonic Poisson's ratio; **PR_Dyn_H**: horizontal dynamic Poisson's ratio; **H_Core_PR_Ultrasonic**: horizontal core ultrasonic Poisson's ratio **PR_Static_V**: vertical static Poisson's ratio; **V_Core_PR**: vertical core static Poisson's ratio; **PR_Static_H**: horizontal static Poisson's ratio; **H_Core_PR**: horizontal core static Poisson's ratio; **Thomsen ξ**: first Thomsen parameter; **Thomsen ϒ**: second Thomsen parameter; **Thomsen δ**: third Thomsen parameter)

As shown in **Fig. 1**. acoustic logs from the sonic scanner tool allowed the estimation of vertical and horizontal dynamic Young's moduli (Ozotta et al., 2021) (YM_Dyn_V) and (YM_Dyn_H) and Poisson's ratios (PR_Dyn_V) and (PR_Dyn_H). The dynamic properties were then converted to the static properties by calibrating against the lab data from a total of 22 core plugs that were tested in both vertical and horizontal directions (two core plugs, one vertical and one horizontal, were taken at each

where the formation exhibits very little to no anisotropy.

4. COMPOSITION AND ELASTIC ANISOTROPY

The elastic anisotropy, as shown in Fig. 1, was magnified in the clay and TOC-rich intervals (Upper and Lower Bakken shales). This can be attributed to the high content of clay minerals and Kerogen. The sheet-like shape of the

main particles of phyllosilicates makes clays inherently anisotropic by having a single preferred orientation. This propensity of single orientation that characterizes phyllosilicates is believed to be a major source of anisotropy in this type of rocks. In contrast, quartz and carbonates show random distributions of the grains leading to more direction independence of the properties of the rocks they form. Wenk et al. (2008) used x-ray goniometry to identify the different mineral phases in the rock as well as their orientations. By Studying different shale samples with multiples of a random distribution (m.r.d) as a quantitative indicator of the tendency of different mineral phases to align themselves in a given orientation inside the rock matrix, as illustrated in **Fig. 2,**they confirmed that phyllosilicates tend to align in the horizontal direction in contrast to the quartz and carbonates minerals that were randomly oriented which is a strong argument that favors the clay as a source of vertical transverse anisotropy.

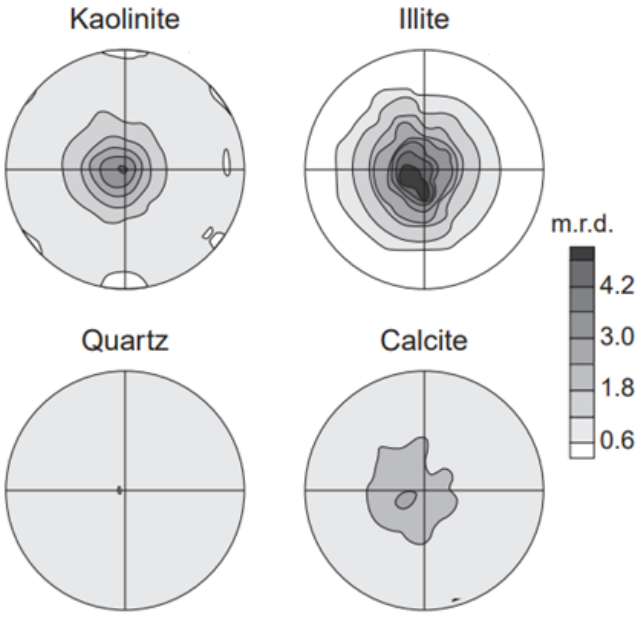

Fig. 2. X-Ray goniometry results for the quantification of preferred mineral orientation using m.r.d. (high m.r.d means a large number of the mineral particle was found in the given orientation) (Wenk et al., 2008).

Another major source of anisotropy in clay and kerogen-rich shales is the presence of high kerogen content (Sayers, 2012). It is widely known that the Kerogen is very soft and complaint compared to the other solid constituents of the rock. The presence of such substance in the matrix composition of the rock can affect its mechanical behavior, especially in very low porosities rocks, which is always the case for unconventional reservoirs. This effect can vary depending on whether the Kerogen is distributed inside the rock matrix in lamination or dispersed form. This can be easily explained if we think of the rock as a binary substance of soft and stiff components, where total clay and Kerogen represent the soft component and the rest of the stiff minerals as the stiff components. The Voigt (iso-strain) and Reuss (Iso-stress) models predict very distinct elastic properties with such an assumption. These models, although often thought of as simple averaging methods, with the binary assumption, they represent the theoretical bounds where the rock is composed of superposed horizontal layers of soft and stiff components. The model assumes that these components are subjected to the same strain in the case of Voigt's model (Iso-strain) (Voigt, 1889) and the same stress in the case of Reuss's model (Iso-Stress) (Reuss, 1929) . In order to examine the effect of clay and Kerogen on the anisotropy of the tested samples, measured vertical and horizontal static Young's moduli from core tests were plotted as a function of clay and kerogen volume fraction, and then, they were compared to Voigt and Reuss's theoretical bounds in addition to Voigt-Reuss-Hill's bound which is the arithmetic average of the two (Hill, 1963). The three bounds were plotted using the values from Sone & Zoback (2013a) with the lowered Young's modulus for the soft components. The lowered Young's modulus for the soft components was used because the SEM images of the Lower Bakken from the study well, shown in **Fig. 3**, proved the existence of porosity in the organic matter particles, which makse the choice of the lowered Young's modulus value for the soft components more representative. This is because the initial reported values were dynamic measurements that can not account for the small pores in the organic matter as argued by the authors.

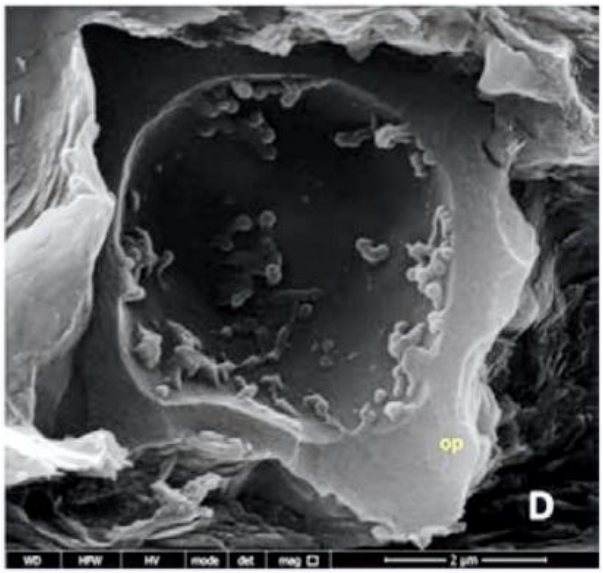

Fig. 3. SEM Image showing porosity presence in the organic matter from the study well (Brinkerhoff et al., 2015).

Fig. 4. Shows that the data presenteda strong correlation between the anisotropy and the clay and kerogen volume fraction. The vertical core results agreed strongly with Reuss's bound, which is what we expect given the previously discussed arguments on the tendency of clays to align horizontally and the tendency of Kerogen to form

very low aspect ratio inclusions and form microcracks along these laminations as discussed in more details in Vernik (1994) and Sayers (2012). Therefore, high clay and Kerogen content with the layered nature of the rock leads to an anisotropic behavior. The observation is in strong agreement with the published data from the other major shale plays in the USA (see for example Sone & Zoback, 2013b).

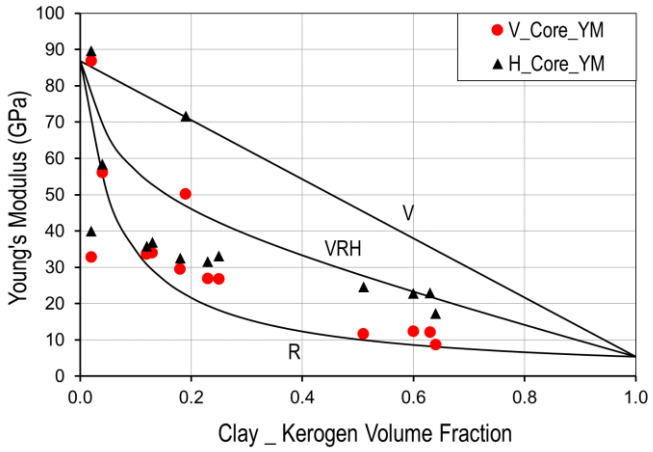

Fig. 4. Static vertical and horizontal cores Young's moduli plotted against the clay_kerogen volume fraction and compared to Reuss, Voigt and Reuss Voigt Hill bounds.

To further understand how the rock fabric and composition relate to the anisotropy of the rock in different members of the Bakken and if the other components are responsible for the observed anisotropy, the solid components of the rock were grouped in three major categories. The stiff components, as referred to earlier, were further subdivided into silicious and carbonates components: 1- QFP (%), which includesthe sum of the weight percentages of quartz, feldspar, and pyrite. This category contains chemically stable stiff minerals.. 2-Carbonates (%), the sum of the weight percentages of all carbonates minerals in the rock such as dolomite, calcite. The minerals in this category are also stiff but are chemically reactive. 3- Clay_ Kerogen (%), which contains the solid components that are believed to be responsible for the anisotropic elastic behavior of the rock (Zoback & Kohli, 2019). To confirm that clay and Kerogen are indeed the only cause of the observed anisotropy, we followed the classification pattern from Sone & Zoback (2013a), where the three categories were plotted on the Ternary diagram, and a color code was applied to the data. Samples having 30% or higher Clay_ Kerogen wt.% were colored in green and considered as Clay _ Kerogen dominated rocks. Samples having 55% or higher QFP wt.% were colored in red and considered as silicious dominated formations, and samples with more than 55 wt.% of carbonates considered carbonates dominated rocks. The rest is considered as mixed mineralogy and was colored in pink.

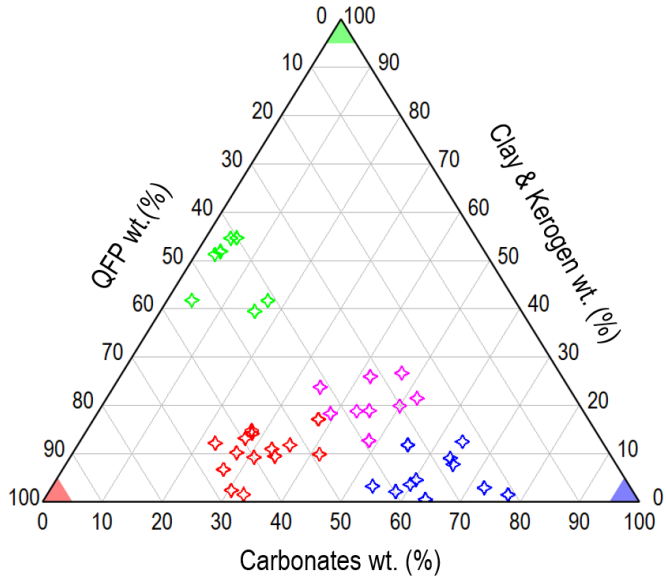

Fig. 5. Ternary diagram classification of cores from study well.

Looking at the ternary diagram and the assigned color codes in a well section view (**Fig. 6**.) together with the Young's modulus and Poisson's ratio anisotropy were plotted (**PR_Anis**: ratio of horizontal to vertical static Poisson's ratio; **YM_Anis**: ratio of horizontal to vertical static Young's modulus), it was confirmed that the anisotropy is indeed only dependent on the clay and kerogen content. Presence of carbonate, silicious or mixed mineralogy dominated constituents appeared not to have a significant effect in terms of anisotropy.

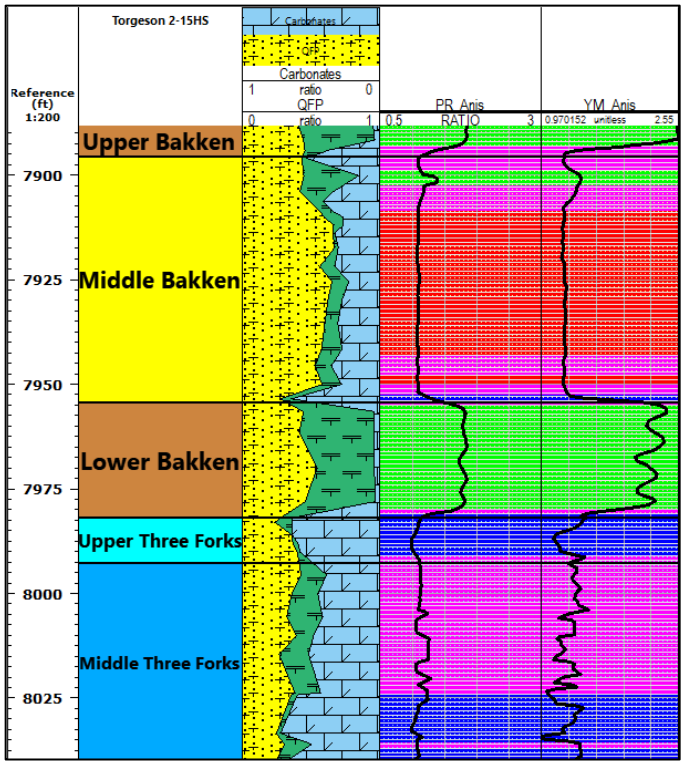

Fig. 6. Well section view to evaluate the effect of different mineral components on the elastic anisotropy of the different formations of The Bakken Petroleum System. (Same color code from Fig. 5. Ternary diagram) (**PR_Anis**: ratio of horizontal to

vertical static Poisson's ratio; **YM_Anis:** ratio of horizontal to vertical static Young's modulus).

5. STRESS MODELING

Commonly, in the oil and gas industry the isotropic extended Eaton's stress model is used to estimate horizontal streswes. In this work, we compared the stress profile prediction from this model to those resulting from a modified version of the extended Eaton's model that accounts for the elastic anisotropy. Comparing these two models, we observed a large contrast between the stress profiles, especially in the clay-rich formations. These observations are due to two main reasons. First, the Poroelastic behavior of the clay-rich formations (Upper and Lower Bakken shales) is very distinct from the pay zones which are characterized by lower clay and TOC content, thus a stiffer matrix. To expand further on this point, the differences in the poroelastic behavior can be quantified using Biot's coefficient. Multiple studies have reported a large contrast between Biot's coefficient in the Upper and Lower Bakken Shales compared to the Middle Bakken and Three Forks members. In this work, a Biot coefficient of α=0.3 was used for the upper and lower Bakken shales and α=0.7 was used for the middle Bakken and Three Forks. These are the values reported in many studies such as Dohmen et al. (2014) and Ling et al. (2016). The difference of Biot's coefficient translates as a smaller contribution of the pore pressure to the minimum horizontal stress in the shaly members compared to the middle Bakken and Upper Three Forks members. The second reason of the large stress contrast between the two models is the elastic anisotropy, which was found to be more pronounced in the shaly members compared to the non-shaly members which exhibit isotropic behavior. For this reason, the use of the anisotropic Eaton's stress model is justified and gives more consistent results with what is usually observed in the field where it is widely observed that formations with high clay and TOC content bear higher horizontal stresses (Upper and Lower Bakken Shales) than the stiffer clay poor formations (Middle Bakken member and Upper Three Forks Member), (Sone & Zoback, 2013b;Mccormack et al., 2021).

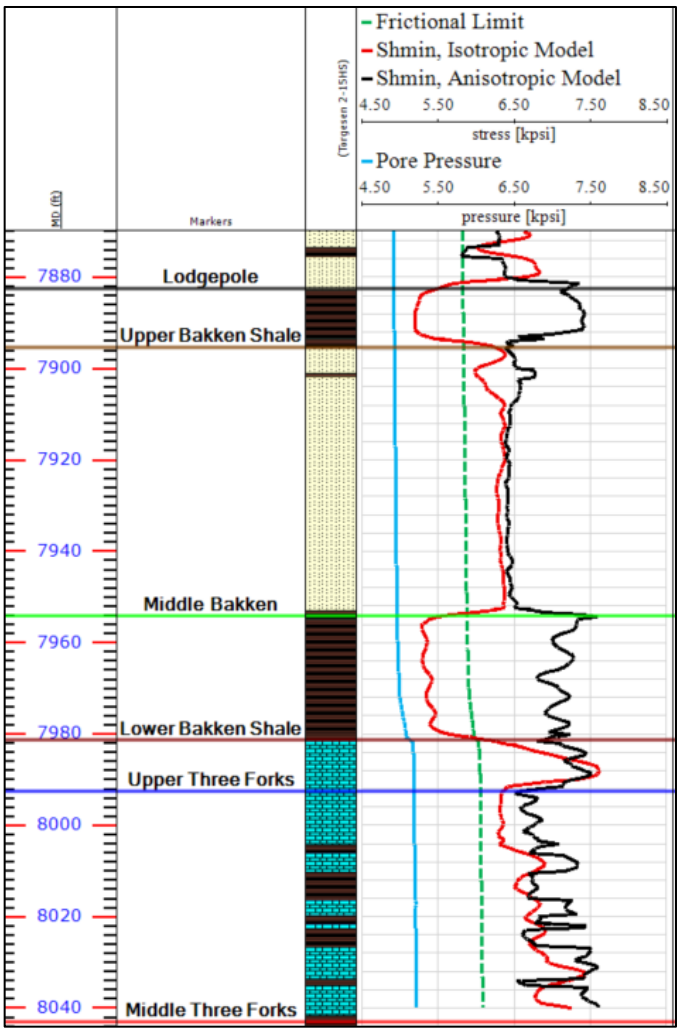

Fig. 7. Stress model for the studied well. Red curve is the minimum horizontal stress estimated from isotropic extended Eaton's stress model. Black curve is the minimum horizontal stress estimated from anisotropic extended Eaton's stress model; Green dashed curve is the frictional limit assuming a friction coefficient μ= 0.6.

6. STRESS CONTRAST

In a normal or strike-slip stress regime (where S_{hmin} is the minimum principal in-situ stress), the contrast of the minimum horizontal in-situ stress (S_{hmin}) between different formations is the main controlling factor on the HF vertical containment. For this particular reason, it is widely known that in order to generate the maximum half-length of the HF, it is necessary to target the intervals with the lowest horizontal S_{hmin}. However, unconventional reservoirs vary in their geological settings, and the HF targeted intervals are not necessarily the intervals with the lowest S_{hmin}. In this case, the desired geometries simply can not be generated because the S_{hmin} contrast between the different layers does not allow the generation of those geometries. In our case sudy, we compare S_{hmin} profiles estimated from

isotropic and anisotropic extended Eaton's stress model to see how they affects the geometry of HF differently.

6.1. Isotropic Stress Model

Using extended Eaton's isotropic stress model, S_{hmin} in the Upper and Lower Bakken shales was predicted to be lower compared to S_{hmin} in the Middle Bakken, which is also lower than that of the Three Forks. In terms of HF geometry, this allowed the induced fracture from the parent well (Upper Three Forks well) **(Fig. 8.A)** to grow in the vertical direction towards the lower Bakken member, with no stress barrier, generating maximum half length in this layer given that it was characterized by a lower S_{hmin} compared to both the underlaying Upper Three Forks member where the fracture was initiated and overlaying Middle Bakken member.

The HF from the infill well (Middle Bakken well) **(Fig.8.B)** propagated mainly in the middle Bakken and Lower Bakken members given that it was initiated in the middle Bakken member, which is relatively thick, and the stress is lower in the Lower Bakken member but higher in the Upper Three Forks member which acted as a stress barrier and therefore the downward propagation of the HF stopped at this depth. Note that significant t half-length was generated in the Bakken three members, the hydraulic fracture height growth was stopped by the Upper Three Forks and lodgepole formations since they had higher S_{hmin} estimates in the isotropic stress model.

6.2. Anisotropic Stress Model

The S_{hmin} profile estimated from extended Eaton's anisotropic stress model gave more realistic results as mentioned earlier since many studies and diagnostic fracture injection test (DFIT) data proved that indeed the stress is highest in the Upper Three Forks, then Upper and Lower Bakken shales were reported to have higher S_{hmin} magnitudes than that of the Middle Bakke member (Dohmen et al., 2014) (Lorwongngam et al., 2018). Using this S_{hmin} profile, the HF from the parent well was found to grow in height towards the Lower Bakken shale and Middle Three Forks. At the same time, half length is generated in the Upper Three Forks member. Once the HF propagates through the Lower Bakken into the middle Bakken, the fracture starts to grow considerably in the Middle Bakken where maximum half length is generated. The lower most part of the Upper Bakken is also hydraulically fractured during the process but it acts as a stress barrier. The HF does not grow past it, given that it has considerably higher stress compared to the Middle Bakken member **(Fig. 8.C)**. The hydraulic fracture from the infill well grows mainly in the middle Bakken, generating considerable half-length. Since a considerably lower S_{hmin} magnitude characterizes the Middle Bakken in this stress profile compared to the Upper and Lower Bakken shale members, these latter act as stress barriers for the HF height growth, which results in forcing the fracture to grow mainly in the middle Bakken with limited propagation in the Upper and Lower Bakken shales.

It is very important to note that in this study, only the growth of one HF was simulated in 4 different scenarios (applies for one perforation cluster per stage design). In case of multiple clusters per stage, the stress shadow can force some of the fractures to grow in the Three Forks due to high-stress shadow in the Middle Bakken in the case of the parent well allowing more oil production from the Upper Three Forks, but it is highly unlikely that the stress shadow can lead the fractures initiated in the Middle Bakken to cross the Upper and Lower Bakken stress barriers.

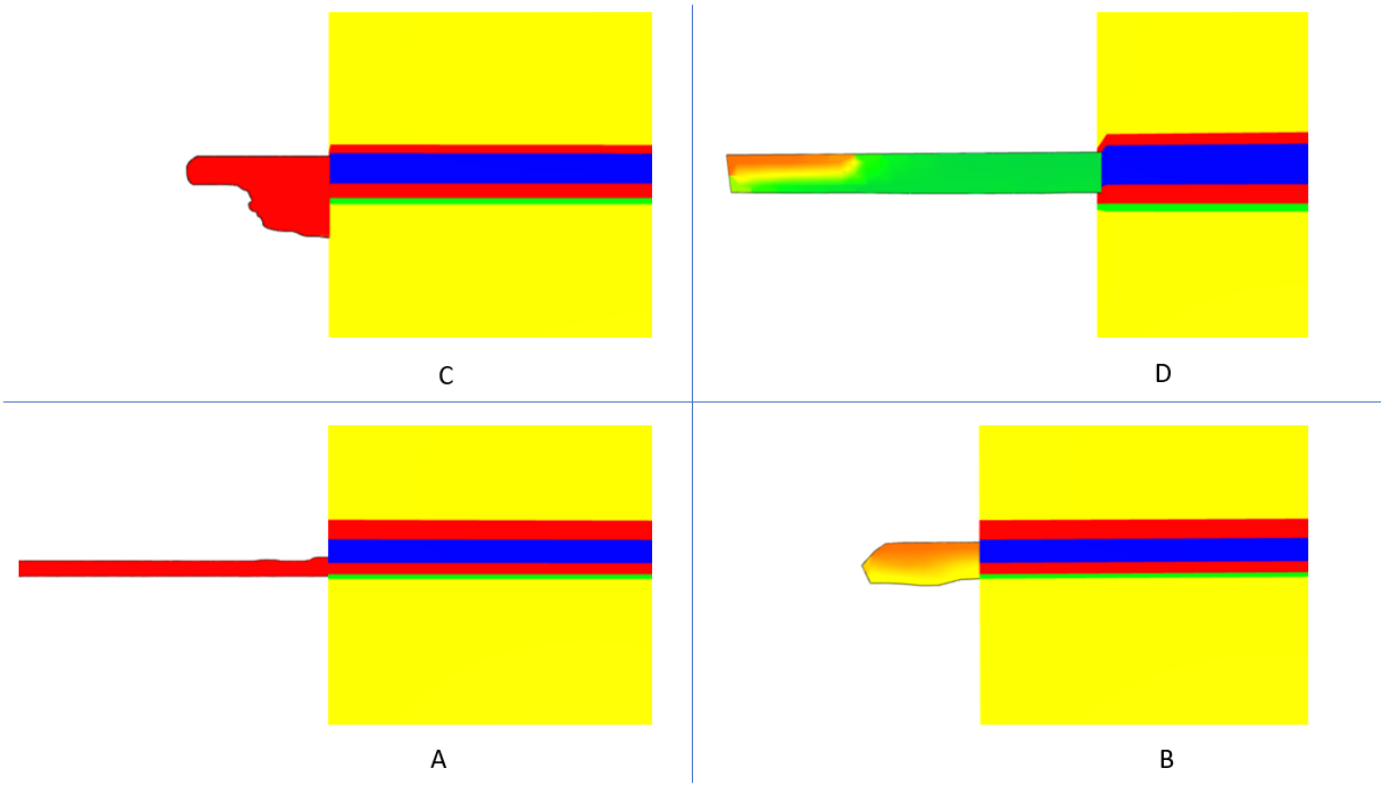

Fig. 8. Hydraulic fracture geometry in four different cases (A: the hydraulic fracturing is performed in the Upper Three Forks and the isotropic stress model was used, B: the hydraulic fracturing is performed in the Middle Bakken and the isotropic stress model was used, C: the hydraulic fracturing is performed in the Upper Three forks and the anisotropic stress model was used, D: the hydraulic fracturing was performed in the Middle Bakken and the)(Yellow: represents the Overlaying Lodgepole formation and the Underlaying Middle Three Forks formations, Red: represents the Upper and Lower Bakken shales, Blue: re[presents the Middle Bakken member, Green: represents the Upper Three Forks Member).

7. CONCLUSIONS

The results of this study demonstrated that the integration of laboratory data with quality logs and understanding the fabric of different layers of an unconventional reservoir and how they affects their mechanical behavior gives higher confidence in the in-situ stress estimation. It was seen that in shale formations with high content of clays and TOC, it is important to use the anisotropic stress model in order to predict the height growth and geometry of the induced fracture correctly. This can lead to high fidelity simulation results that can be implemented successfully to understand what is happening in the subsurface. Once the different phenomena in the subsurface are understood, the optimization of the hydraulic fracturing and well spacing becomes more meaningful as it is based on a solid scientific base.

ACKNOWLEDGMENT

The authors would like to acknowledge the North Dakota Industrial Commission (NDIC) for the financial support of this work through contract NDIC G-045-89. We are also grateful to ResFrac Corporation, Schlumberger, and Baker Hughes for supporting this study with the use of their commercial software.

REFERENCES

1. Anna, L. O., Pollastro, R., & Gaswirth, S. B. (Usgs). (2010). Williston Basin Province — Stratigraphic and Structural Framework to a Geologic Assessment of Undiscovered Oil and Gas Resources. *Assessment of Undiscovered Oil and Gas Resources of the Williston Basin Province of North Dakota, Montana, and South Dakota, 2010*, Chapter 2/7.
2. Brinkerhoff, R., Fluckiger, S., Millard, M., & Walls, J. (2015). Hydrocarbon contribution from the Lower Bakken Shale in horizontal wells drilled in the Three Forks

Formation in Divide County, ND. *Society of Petroleum Engineers - Unconventional Resources Technology Conference, URTeC 2015*, 1–8. https://doi.org/10.2118/178556-ms

3. Chemmakh, A. (2021). Machine learning predictive models to estimate the UCS and tensile strength of rocks in Bakken Field. *Proceedings - SPE Annual Technical Conference and Exhibition*, *2021-Septe*. https://doi.org/10.2118/208623-STU
4. Dohmen, T., Blangy, J. P., & Zhang, J. (2014). Microseismic depletion delineation. *Interpretation*, *2*(3), SG1–SG13. https://doi.org/10.1190/INT-2013-0164.1
5. Ellafi, A., Jabbari, H., Geri, M. B., & Alkamil, E. (2019). *SPE-197744-MS Can HVFRs Increase the Oil Recovery in Hydraulic Fractures Applications ? Bakken Petroleum System (BPS), Williston Basin*.
6. Frydman, M., Pacheco, F., Pastor, J., Canesin, F. C., Caniggia, J., & Davey, H. (2016). Comprehensive determination of the far-field earth stresses for rocks with anisotropy in tectonic environment. *Society of Petroleum Engineers - SPE Argentina Exploration and Production of Unconventional Resources Symposium*, 1–14. https://doi.org/10.2118/180965-ms
7. Ganpule, S., Srinivasan, K., Izykowski, T., Luneau, B., & Gomez, E. (2015). Impact of geomechanics on well completion and asset development in the Bakken formation. *Society of Petroleum Engineers - SPE Hydraulic Fracturing Technology Conference 2015*, 64–79. https://doi.org/10.2118/173329-ms
8. Hill, R. (1963). Elastic properties of reinforced solids: Some theoretical principles. *Journal of the Mechanics and Physics of Solids*, *11*(5), 357–372. https://doi.org/10.1016/0022-5096(63)90036-X
9. LEFEVER, J. A., North Dakota Geolog. (1992). Petroleum Potential of the Middle Member, Bakken Formation, Williston Basin. *AAPG Bulletin*, *76*, 74–94. https://doi.org/10.1306/f4c900ce-1712-11d7-8645000102c1865d
10. Ling, K., He, J., Pei, P., Wang, S., & Ni, X. (2016). Comparisons of Biot's coefficients of bakken core samples measured by three methods. *50th US Rock Mechanics / Geomechanics Symposium 2016*, *2*(February 2017), 1603–1615.
11. Lorwongngam, A. O., Cipolla, C., Gradl, C., Cidoncha, J. G., & Davis, B. (2018). Multidisciplinary data gathering to characterize hydraulic fracture performance and evaluate well spacing in the Bakken. *Society of Petroleum Engineers - SPE Hydraulic Fracturing Technology Conference and Exhibition 2019, HFTC 2019*. https://doi.org/10.2118/194321-ms
12. Ma, X., & Zoback, M. D. (2017). Laboratory experiments simulating poroelastic stress changes associated with depletion and injection in low-porosity sedimentary rocks. *Journal of Geophysical Research: Solid Earth*, *122*(4), 2478–2503. https://doi.org/10.1002/2016JB013668
13. Mccormack, K. L., Zoback, M. D., & Kuang, W. (2021). A case study of vertical hydraulic fracture growth, stress variations with depth and shear stimulation in the Niobrara Shale and Codell Sand, Denver-Julesburg Basin, Colorado. *Interpretation*, *9*(4), SG59–SG69. https://doi.org/10.1190/INT-2020-0246.1
14. McKimmy, M., Hari-Roy, S., Cipolla, C., Wolters, J., Jackson, H., & Kyle, H. (2022). *Hydraulic Fracture Geometry, Morphology, and Parent-Child Interactions: Bakken Case Study*. https://doi.org/10.2118/209162-ms
15. Ozotta, O., Ostadhassan, M., Rasouli, V., Pu, H., Malki, M. L., Dawodu, O. V., & Kolawole, O. (2021). Homogenization Models to Determine the Change in Elastic Properties Due to CO2 Injection. *55th U.S. Rock Mechanics / Geomechanics Symposium 2021*, *1*(June), 600–609.
16. Ozotta, O., Malki, M. L., Rasouli, V., & Pu, H. (2021). *ARMA / DGS / SEG International Geomechanics Symposium The Effect of Pore Morphology on Fracture Systems*. *November*.
17. Reuss, A. (1929). Berechnung der Fließgrenze von Mischkristallen auf Grund der Plastizitätsbedingung für Einkristalle . *ZAMM - Journal of Applied Mathematics and Mechanics / Zeitschrift Für Angewandte Mathematik Und Mechanik*, *9*(1), 49–58. https://doi.org/10.1002/zamm.19290090104

18. Sayers, C. M. (2012). The effect of kerogen on the elastic anisotropy of organic-rich shales. *Geophysics*, *78*(2), D65–D74. https://doi.org/10.1190/GEO2012-0309.1
19. Sone, H., & Zoback, M. D. (2013). Mechanical properties of shale-gas reservoir rocks - Part 1: Static and dynamic elastic properties and anisotropy. *Geophysics*, *78*(5). https://doi.org/10.1190/GEO2013-0050.1
20. Sone, H., & Zoback, M. D. (2013). Mechanical properties of shale-gas reservoir rocks - Part 2: Ductile creep, brittle strength, and their relation to the elastic modulus. *Geophysics*, *78*(5). https://doi.org/10.1190/GEO2013-0051.1
21. Sonnenberg, S. a, Gantyno, A., & Sarg, R. (2011). Petroleum Potential of the Upper Three Forks Formation , Williston Basin , USA *. *Petroleum Geology*, *110153*.
22. Theloy, C. (2014). *Integration of Geological and Technological Factors Influencing Production in the Bakken Play, Williston Basin*. 151–156. http://hdl.handle.net/11124/233
23. Vernik, L. (1994). Hydrocarbon-generation-induced microcracking of source rocks. *Geophysics*, *59*(4), 555–563. https://doi.org/10.1190/1.1443616
24. Voigt, W. (1889). Ueber die Beziehung zwischen den beiden Elasticitätsconstanten isotroper Körper [On the relationship between the two elastic constants of an isotropic body]. *Annalen Der Physik*, *274*(12), 573–587.
25. Wenk, H. R., Voltolini, M., Mazurek, M., Van Loon, L. R., & Vinsot, A. (2008). Preferred orientations and anisotropy in shales: Callovo-oxfordian shale (France) and opalinus clay (Switzerland). *Clays and Clay Minerals*, *56*(3), 285–306. https://doi.org/10.1346/CCMN.2008.0560301
26. Zoback, M. D., & Kohli, A. H. (2019). Unconventional Reservoir Geomechanics. In *Unconventional Reservoir Geomechanics*. Cambridge University Press. https://doi.org/10.1017/9781316091869